

## MIT Open Access Articles

*Can oceanic flows be heard? Abyssal melodies*

The MIT Faculty has made this article openly available. **Please share** how this access benefits you. Your story matters.

**Citation:** Wunsch, Carl. 2022. "Can oceanic flows be heard? Abyssal melodies." 152 (4).

**As Published:** 10.1121/10.0014603

**Publisher:** Acoustical Society of America (ASA)

**Persistent URL:** <https://hdl.handle.net/1721.1/146977>

**Version:** Final published version: final published article, as it appeared in a journal, conference proceedings, or other formally published context

**Terms of use:** Creative Commons Attribution 4.0 International license



## Can oceanic flows be heard? Abyssal melodies

Carl Wunsch

Citation: [The Journal of the Acoustical Society of America](#) **152**, 2160 (2022); doi: 10.1121/10.0014603

View online: <https://doi.org/10.1121/10.0014603>

View Table of Contents: <https://asa.scitation.org/toc/jas/152/4>

Published by the [Acoustical Society of America](#)

---

### ARTICLES YOU MAY BE INTERESTED IN

[Shallow-water waveguide acoustic analysis in a fluctuating environment](#)

The Journal of the Acoustical Society of America **152**, 1252 (2022); <https://doi.org/10.1121/10.0013831>

[A wave glider-based, towed hydrophone array system for autonomous, real-time, passive acoustic marine mammal monitoring](#)

The Journal of the Acoustical Society of America **152**, 1814 (2022); <https://doi.org/10.1121/10.0014169>

[Long-term noise interferometry analysis in the northeast Pacific Ocean](#)

The Journal of the Acoustical Society of America **151**, 194 (2022); <https://doi.org/10.1121/10.0009232>

[Rayleigh limit extended: Scattering from a fluid sphere](#)

The Journal of the Acoustical Society of America **152**, R7 (2022); <https://doi.org/10.1121/10.0014345>

[The beginning of time-frequency analysis](#)

The Journal of the Acoustical Society of America **152**, R9 (2022); <https://doi.org/10.1121/10.0014987>

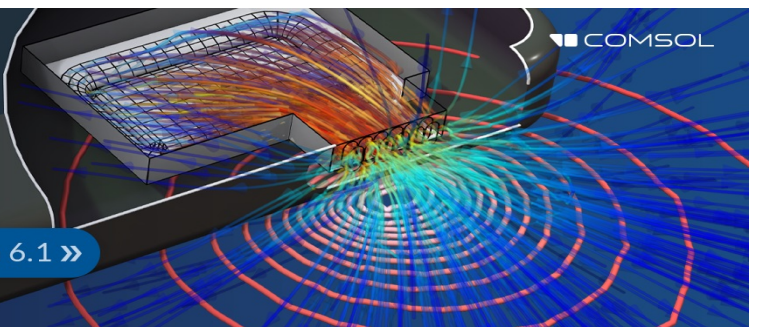
[Acoustic scattering and the exact Green function](#)

The Journal of the Acoustical Society of America **152**, 2038 (2022); <https://doi.org/10.1121/10.0014346>


---

**High-fidelity modeling.  
Reliable results.**

Simulate with COMSOL Multiphysics® version 6.1 »



## Can oceanic flows be heard? Abyssal melodies

Carl Wunsch<sup>a)</sup> 

Department of Earth and Planetary Sciences, Harvard University, Cambridge, Massachusetts 02138, USA

### ABSTRACT:

Fluid flows generate an acoustic noise field. In principle, oceanic flows on varying time and length scales produce a sound field and its detectability is considered here. A fragile lower bound analysis is made of the acoustic signature, using the Lighthill theory, of a simple train of boundary vortices generated by baroclinic tidal flows. Subject to numerous assumptions, the accompanying sound should be detectable within the hum band of seismo-acoustic pressure fields, and more generally, across the entire oceanic spectrum—likely through wave number analyses of spatially coherent acoustic array data. © 2022 Author(s). All article content, except where otherwise noted, is licensed under a Creative Commons Attribution (CC BY) license (<http://creativecommons.org/licenses/by/4.0/>).

<https://doi.org/10.1121/10.0014603>

(Received 1 April 2022; revised 18 September 2022; accepted 19 September 2022; published online 13 October 2022)

[Editor: Oleg A. Godin]

Pages: 2160–2168

### I. INTRODUCTION

This note began as an attempt at understanding a simply posed question: can the ocean circulation, its associated turbulence, and its changes through time be heard? The question has both some interesting mathematical aspects and some potentially interesting and important practical aspects. It does not appear to be a subject with an extended literature. A large oceanic literature exists on the impact of fluid flow structures on ambient sound (e.g., sonar and whale signals), but little or nothing seems known about the sounds generated by the flows themselves. See any of numerous textbooks including Jensen *et al.* (2011), Medwin and Blue (2005), and Colosi (2015).

It is well known that turbulence can generate noise. When the question is applied to the ocean, several more questions are encountered: (1) Is the sound detectable with existing instruments? (2) Is the sound detectable in the presence of background noise? (3) Is the level of turbulence sound significant relative to the generation of Earth hum, for example (Webb, 2008; Chave *et al.*, 2019)? (4) Is the inverse problem of determining the source characteristics solvable? To save some readers much time, the simple conclusion to all of these questions remains a speculative “maybe”, but they are worth reviewing because (a) of the large number of assumptions necessary for the calculation; (b) of the great parameter sensitivity in parts of it—encompassed in large measure by the far-field “Lighthill’s 8th power law” in the flow velocity; (c) it could lead to a comparatively cheap, passive, global ocean observing system; and (d) some interesting mathematics is involved. Answering these questions proves remarkably complicated, considering the mathematical complexities of even the simplest forms of oceanic turbulence. The present note is directed at obtaining

approximate amplitude levels and their frequency structure of a much simplified situation—with no intention of being definitive. The editor (O. Godin) and a reviewer have concluded that the effects are likely undetectable, but an effort has been made here to consistently find lower bounds on the sound generation. In any case, coherent spatial arrays, not individual hydrophones, would be used for detection as explained below.

Ocean “noise” has been measured for many decades (e.g., Wenz, 1962, is a classical reference). Most recent attention has been on high frequency trends owing to changes in shipping noise, seismic exploration, ice sheet breakup, etc., and in the understanding of biological phenomena through their emissions and ecological responses to sound field changes. These ocean acoustics measurements have tended to focus on the sound field between order 100 Hz and many kilohertz. At the lower end of the spectrum, at fractions of 1 Hz, seismic data are encountered, including those used for earthquake detection (e.g., Wu *et al.*, 2020) and the subject of microseisms and Earth “hum” (e.g., Webb, 2008; Nishida, 2013; Diaz, 2016). That subject is not without controversy (Ardhuin and Herbers, 2013, is a good starting point). Active and passive source ocean acoustic tomography (Munk *et al.*, 1995; Howe *et al.*, 2019) has tended to focus on frequencies of order 10–100 Hz where the dissipation is treated as negligible.

A large body of literature exists on the complex ocean energy spectral cascades, both forward and backward, in wavenumber,  $k$ , space (Ferrari and Wunsch, 2009; Arbic *et al.*, 2014; Vallis, 2017). Those wavenumbers have spatial scales ranging from the order of the width of the Pacific Ocean ( $10^7$  m) to the viscous dissipational scale  $<10^{-2}$  m. Some significant fraction of the total energy sustaining the oceanic flow field (not all) is believed dissipated through a wavenumber cascade, perhaps ending ultimately in a classical Kolmogorov  $k^{-5/3}$  spectrum inertial subrange and viscous cutoff. The intense diapycnal mixing of the ocean is

<sup>a)</sup>Also at: Department of Earth, Atmospheric and Planetary Sciences, MIT, Cambridge MA 02139, USA. Electronic mail: carl.wunsch@gmail.com

believed to depend directly upon provision of energy to the centimeter and smaller scale wavenumbers (e.g., Thorpe, 2005; Arbic *et al.*, 2009; Gregg, 2021; Moum, 2021). Time scales are generally much longer than any that are normally included in acoustic or seismic studies. It remains uncertain how much occurs in the open ocean and how much is confined to boundary regions.

Energy input into large-scale oceanic flows is on the order of  $2 \times 10^{12}$  W (2TW). That includes energy from the wind field, baroclinic tidal generation, heating–cooling, and associated atmospheric forcings, but not the energy in the purely barotropic tidal motions or in surface gravity waves (see Ferrari and Wunsch, 2009, and Table II in Wunsch, 2020). Ultimately, this energy must be dissipated on the viscous scales, although some (poorly known) fraction will occur in the complexity of continental-shelf boundary processes involving numerous wave transformations. Does any of this energy emerge in the normal seismo-acoustic bands?

Many assumptions follow below, and the results should be regarded as a preliminary scale analysis as a step towards formulating questions, rather than answering them. It will become plain that some of the numbers obtained can have errors of orders of magnitude.

## A. Units

This subject exists in the overlap of ocean acoustics of biology, anti-submarine warfare, seismology, shipping, and physical oceanography of all kinds, with conflicting notations and assumptions leading to some translation problems, of which time scale units are important. Some seismo-acoustic data are presented in  $\mu\text{Hz}$  and  $\text{mHz}$ , and some acoustic data are in  $\text{kHz}$ . Formally, ocean pressure variations are of interest in a frequency range that might run from the Milankovitch cycles of period of order  $10^5$  y ( $3 \times 10^{-13}$  Hz) and longer, to the use of biological sounds at 200 kHz ( $2 \times 10^5$  Hz; e.g., Haver *et al.*, 2018), or more than 18 orders of magnitude. For convenience, Table I produces some equivalents between oceanographers' period units, such as hours or days, to seismic/acoustic frequencies in Hertz (Hz) along with accompanying acoustic field wavelengths. Seismic and ocean acoustic interests overlap roughly from 0.1–100 Hz, with acoustics having a focus at higher frequencies, and seismology and geophysics generally, at the lower frequencies. Still lower frequencies are dominated by the non-compressible pressure physics of the oceanic flows, but which will have radically different wavenumbers from the compressible acoustic component. A crossover may exist at high frequencies where the compressible motions dominate. In any observational test, the wavenumber spectra of the acoustic motions will likely be the mechanism by which the complex set of pressures (many being hydrostatic) generators of ocean pressures will be able to distinguish motions owing to oceanic hydrodynamic and seismic phenomena from their generated acoustic fields.

Oceanographic pressures are commonly given in equivalent surface elevations of centimeters or meters or more

TABLE I. Correspondence between oceanographic and seismic/acoustic time intervals and frequencies. Note that sound will have twice the hydrodynamic generating frequency and half the wavelength in the simple case considered here. Solid Earth free oscillations occur at periods shorter than approximately 1 h, with the Earth hum band sometimes defined as here. Because of the large sound speed value, acoustic wavelengths are generally much larger than the generating hydrodynamic wavelengths, in principle permitting observational separation in wavenumber space.

Period (days, h, min, s)	Frequency, s (cps, Hz)	Frequency, s ( $\mu\text{Hz}$ )	Acoustic wavelength (m)
1 day = 24 h	$1.16 \times 10^{-5}$	11.6	$1.3 \times 10^8$
$M_2$ tide, 12.42 h	$2.24 \times 10^{-5}$	22.4	$6.7 \times 10^7$
1 h	$2.78 \times 10^{-4}$	278	$5.4 \times 10^6$
1 min	$1.7 \times 10^{-2}$	$1.7 \times 10^4$	$88 \times 10^3$
1 s = $2.8 \times 10^{-4}$ min	1.0	$10^6$	$1.5 \times 10^3$
Earth hum band: 300–30 s (Diaz, 2016)	$3 \times 10^{-3}$ – $3 \times 10^{-2}$	$3 \times 10^3$ – $3 \times 10^4$	$(455\text{--}50) \times 10^3$
Microseism band: 25–1 s (Diaz, 2016)	0.04–1	$4 \times 10^4$ – $10^6$	$(38\text{--}1.5) \times 10^3$

formally in Pascals (Pa) for which  $1 \text{ Pa} = 1 \text{ kg}/(\text{m}\cdot\text{s}^2)$ . The incompressible pressure,  $g\rho_0\eta$ , of  $\eta = 1$  cm of sea level elevation with a density of  $\rho_0 \approx 10^3 \text{ kg}/\text{m}^3$ ,  $g \approx 10 \text{ m}/\text{s}^2$  is about  $10^2$  Pa (1 hPa). In acoustics and seismology,  $\mu\text{Pa}$  are common units, and so 1 cm of sea level elevation is  $\approx 10^8 \mu\text{Pa}$ . Much of ocean acoustics generally is expressed on a decibel scale (e.g., Jensen *et al.*, 2011),  $20 \log_{10}(p/p_{\text{ref}})$  where  $p_{\text{ref}} = 1 \mu\text{Pa}$ . In this paper, in the interests of simplicity, only Pascals and Hertz are used mostly. The significance of the long acoustic wavelengths at any given frequency lies with their orders of magnitude difference to those of any underlying fluid flow.

The question now is whether the sound pressures radiated by oceanographic flows are sufficiently intense to be observable in frequency space? Answering the question involves the intensity of generation, the sensitivity of instruments, and the levels of other sound sources present. The context of sensitivity and of the background noise is usefully examined in Fig. 1, the same as Fig. 1 of Chave *et al.* (2019), as an example. That figure displays, in hertz, the spectral density from a pressure instrument (see Filloux, 1980) deployed on the seafloor near Hawaii over an interval of 2 months. The strong tidal oscillations, ranging from the diurnal through various over-tides for approximately 1 h, are conspicuous in the pressure spectral density estimate. A low-frequency continuum exists, becoming white-noise at the lowest frequencies, and with a red-noise continuum above the tides, falling until the hum band is encountered between about  $3 \times 10^{-3}$  and  $10^{-2}$  Hz (300–30 s) and then falling to the noise floor above. A microseism band believed generated by non-linear interacting surface gravity waves (infragravity waves, IGW) lies just above the frequencies shown. The power density range is over 10 orders of magnitude. Power in the diurnal and semidiurnal tides dominates the entire frequency spectrum as is made clear by Fig. 2, which shows the cumulative power with frequency.



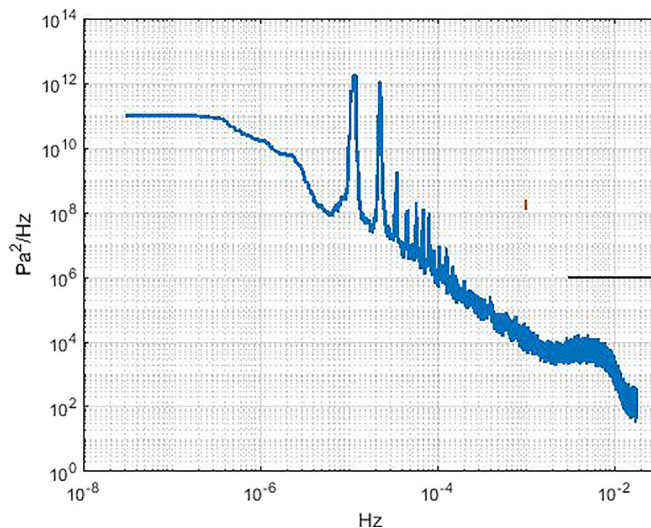


FIG. 1. (Color online) Multitaper spectral density estimate of bottom pressure (Chave *et al.*, 2019) using an instrument described in Filloux, 1980) from a record NNW of Kauai in the Hawaiian Islands in 5235 m of water (26°52'N, 161°57'W). Tidal lines as well as the microseism energy excess are visible. Electromagnetic effects and conventional overtones are also present there. This result is a recomputation, in  $\text{Pa}^2/\text{Hz}$  and  $\text{Hz}$ , nearly indistinguishable, from Fig. 1 in Chave *et al.* (2019). Time-bandwidth product in the multitaper estimate here is 6.5. The horizontal line is approximately the hum band as defined by Diaz (2016) and which extends to even higher frequencies. A frequency-averaged approximate 95% confidence interval is shown in the vertical bar and is visibly relevant only to the lowest frequencies.

An equivalent spectrum from a DART instrument is shown in Fig. 3 in units of  $\text{Pa}$  and  $\text{Hz}$ . {The DART website describes it: “As part of the U.S. National Tsunami Hazard Mitigation Program (NTHMP), the Deep Ocean Assessment and Reporting of Tsunamis [DART(R)] Project is an ongoing effort to maintain and improve the capability for the early detection and real-time reporting of tsunamis in the open ocean. DART(R) stations have been sited in regions with a history of generating destructive tsunamis to ensure early detection of tsunamis and to acquire data critical to real-time forecasts. DART(R) systems consist of an anchored seafloor bottom pressure recorder (BPR) and a companion moored

surface buoy for real-time communications. An acoustic link transmits data from the BPR on the seafloor to the surface buoy. The data are then relayed via an Iridium satellite link to ground stations, which demodulate the signals for immediate dissemination to National Oceanographic and Atmospheric Administration’s Tsunami Warning Centers, National Data Buoy Center, and Pacific Marine Environmental Laboratory.”} For reference, the total power in the frequency band above about  $10^{-3}$   $\text{Hz}$  in the DART spectrum is of order  $5000\text{Pa}^2/\text{Hz} \times 0.005 \text{ Hz} = 25\text{Pa}^2 = 5\text{Pa RMS}$ —about 0.05 cm of water equivalent). The background spectral density values near  $10^{-3}$   $\text{Hz}$  are approximately  $10^3 \text{ Pa}^2/\text{Hz}$ . With the present resolution of  $1.5 \times 10^{-8}$   $\text{Hz}$ , any line or narrowband process with an energy above a frequency of  $1 \times 10^{-2}$   $\text{Hz}$ , exceeding about  $1.5 \times 10^{-5} \text{ Pa}^2$  or  $4 \times 10^{-3}$   $\text{Pa}$  root mean square (RMS), would stand above the background and this value might be taken as a minimal reference value of importance for such a process.

At higher frequencies, microseisms and many types of manmade and biological noise sources come to dominate. Chave *et al.* (2019) focus on excitation in this relatively quiet energy band by solar modal excitation via the geomagnetic fields and by hydrostatic tidal overtones, but for present purposes, a question is whether some of this energy cannot also be accounted for by oceanic fluid flows? The hum band consists, at least in part, of the ongoing excited normal modes of the solid Earth (see, e.g., Webb, 2008; Diaz, 2016; Chave *et al.*, 2019). Above the tidal harmonics, the spectral density is remarkably structured, as can be noticed in the spectral range relative to the approximate 95% confidence interval. When displayed at higher resolution (not shown), many isolated peaks appear above a noisy background. Sources of the visible peaks at the very highest frequencies are not known.

Much attention lies in the high frequency end of these spectra where it becomes of interest in seismic and nonlinear water wave problems. The spectral range of  $10^{11}\text{Pa}^2/\text{Hz}$  suggests a severe challenge to the assumptions of linearity in the system and the absence of significant spectral leakage in the estimates.

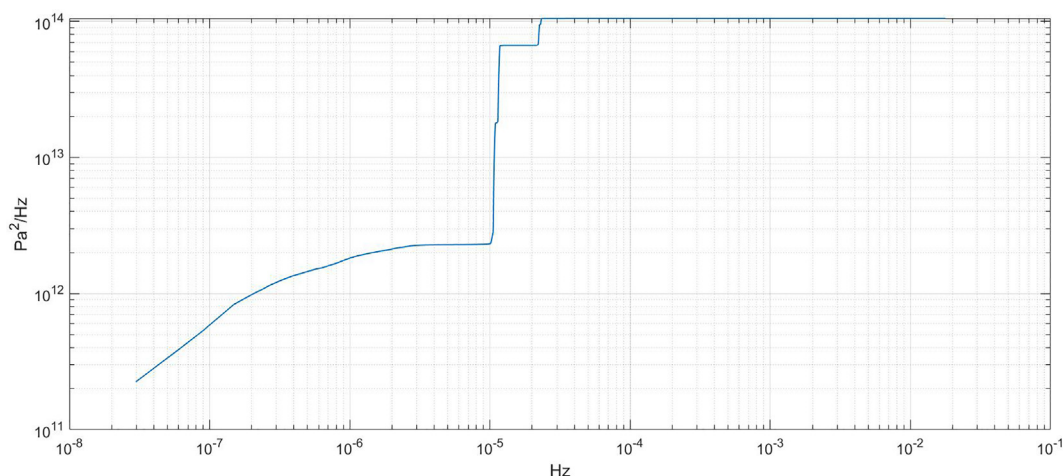


FIG. 2. (Color online) Cumulative sum of the power density of Fig. 1 showing the tidal dominance of the power. Step changes correspond to the diurnal and semi-diurnal bands. Seismic and microseism attention tends to lie in the relatively very low energy band at the highest frequencies.

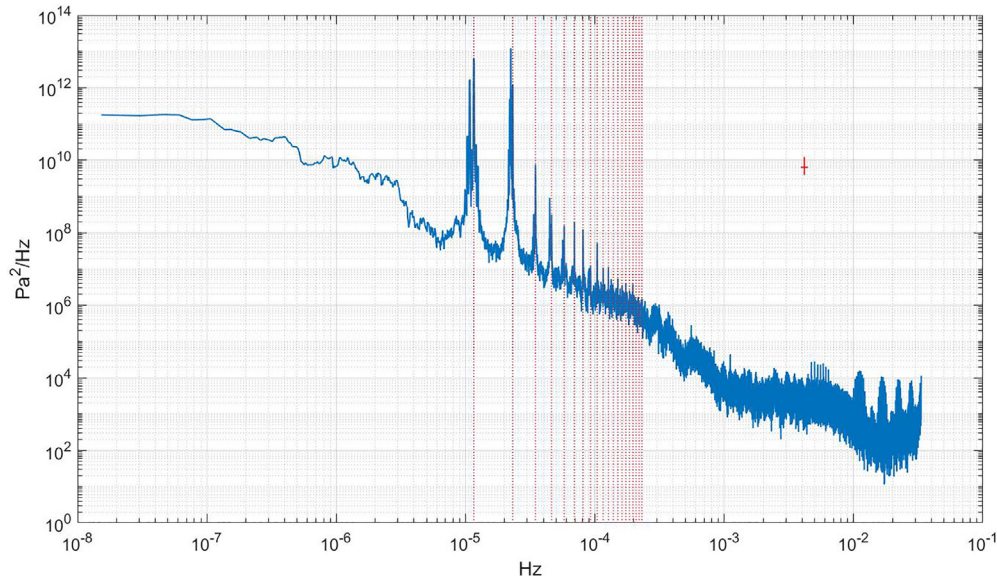


FIG. 3. (Color online) DART multitaper spectrum from 19.556°N 156.538°W 4700 m, near Hawaii, in  $\text{Pa}^2/\text{Hz}$  and  $\text{Hz}$  also showing the principal solar tide  $S_1$  and its first nine harmonics (vertical dashed lines). No immediate explanation is offered for the peaks at the very high end of the spectrum. The record length is 2 y at time intervals of 15 s. Pressure is that observed, regardless of whether the source is of hydrodynamic or acoustic origin. Vertical line is an approximate mean 95% confidence interval, but seemingly not relevant at the highest frequencies present.

## II. SOUND GENERATION IN A FLUID

This subject, in English, begins with two papers by Lighthill (1952, 1954) who showed that noise generation by fluid flows at small Mach number and large Reynolds number originated with the quadrupole-moments of the flow field. In the many intervening decades, the field has grown vigorously, with a major focus on aircraft noise generation. Proudman (1952) and Kraichnan (1957) applied the theory to a problem of relevance here—sound generation by homogeneous turbulence—albeit whether anything in the ocean is homogeneous is doubtful. It becomes immediately clear that answers to the questions posed above in Sec. I will depend upon whether the observing instrument lies within the turbulence itself, or is in the far-field or likely, both simultaneously.

In what follows here, the author has relied on textbooks for discussion of the fundamental physics (Morse and Ingard, 1968; Monin and Yaglom, 1975; Howe, 2003). For the present purposes, the limit of interest is that of very high Reynolds number,  $Re$ , and near-vanishing Mach number,  $M = u/c_a$ , where  $c_a$  is the speed of sound in seawater, and  $u$  is an RMS hydrodynamic velocity. A fundamental and justified assumption, used throughout here, is that the power lost (energy loss) to the acoustic field is a negligible part of the energy and power of the hydrodynamic flow. Following, e.g., a distinction is made between the *hydrodynamic pressure* (Morse and Ingard, 1968),  $p_h$ , and the *acoustic pressure*,  $p_a$ . In the Lighthill theory that ignores viscous effects on the sound generation, the wave equation for the perturbation density field associated with the acoustic pressure in this limit, is (Eq. 2.1.12 in Howe, 2003)

$$\left(\frac{1}{c_a^2} \frac{\partial^2}{\partial t^2} - \nabla^2\right) p_a = \sum_{i,j=1}^3 \frac{\partial^2 T_{ij}(\mathbf{r}, t)}{\partial x_i \partial x_j} \text{kg}/(\text{m}^3 \text{s}^2) \\ = \mathcal{F}(x, y, z, t) \quad (1)$$

in three Cartesian dimensions,  $\mathbf{r} = [x, y, z]^T = [x_1, x_2, x_3]^T$ , and time  $t$ . The term on the right is the double divergence of the acoustic quadrupole-moment generating function. Lighthill's tensor,  $T_{ij}$ , in this limit depends on the Reynolds stresses, where  $u_i$ ,  $i = 1, 2, 3$  are the three components of velocity (MLH, P. 30) and is

$$\mathbf{T} = \{T_{ij}(x, y, z, t)\} \\ \approx \{\rho_0 u_i(x, y, z, t) u_j(x, y, z, t)\} \text{kg}/(\text{m} - \text{s}^2), \\ i, j = 1, 2, 3 \quad (2)$$

with the mean density,  $\rho_0$ , included. Velocities are all hydrodynamic. The corresponding acoustic pressure is

$$p_a = p_0 + c_a^2 \rho_a \text{kg}/(\text{m} - \text{s}^2), \quad (3)$$

$p_0$  from the mean density  $\rho_0$ . In this paper,  $p_a$  and  $\rho_a$  will be re-defined as perturbations based on these reference values.

This development ignores acoustic dissipation, which is weak at the low frequencies of interest here (e.g., Munk et al., 1995; Jensen et al., 2011). Much of the difficulty of this subject arises from the presence of boundaries and complicated shear flows (Möhring, 1979, and other papers in Müller, 1979). When the hydrodynamic field is that of a pure radian frequency  $\sigma_h = 2\pi s_h$ , Eq. (1) becomes the three-dimensional Helmholtz equation,

$$\nabla_3^2 p_a + \frac{(2\sigma_h)^2}{c_a^2} p_a = \sum_{i,j=1}^3 \frac{\partial^2 T_{ij}(\mathbf{r}, \sigma_h)}{\partial x_i \partial x_j} \text{kg}/(\text{m}\cdot\text{s}^2) \\ = F(x, y, z, \sigma_h). \quad (4)$$

The statistics of  $\mathbf{T}$ , its derivatives, and the products of its elements are needed to calculate power generation, covariances, and spectra. A simple implication of Eq. (4) is that  $p_a$  is unlikely to have a normal probability distribution. Indeed, if the velocity field is Gaussian as commonly assumed,  $\mathbf{T}$  would have a non-central  $\chi^2$  distribution. The purpose of this paper is to obtain, through the (perhaps) simplest possible configurations, some order of magnitude, lower-bound estimates of the  $p_a$  and their frequency distribution.

### A. Far-Field

Much of the literature is devoted to the far-field behavior of a sound source. The results demonstrate the extreme sensitivity the acoustic field has to details of the flow, potentially useful in actual measurement, but a challenge to theory. The Lighthill far-field construct assumes the listener lies outside the region of turbulence itself—in an otherwise resting *three-dimensional* fluid. Let  $L$  be a characteristic length scale in a vorticity-containing eddy,  $u$  is the typical velocity within an eddy, and  $\tau \approx L/u$  is a characteristic time scale. Then, the far-field pressure,  $p_{FF}$  from one isotropic eddy with *spherical* spreading of acoustic energy is

$$p_{FF} \approx \frac{L}{|\mathbf{r}|} \rho_0 u^2 M^2 \text{Pa} = \frac{L}{c_a^2 |\mathbf{r}|} \rho_0 u^4 \quad (5)$$

(Howe, 2003), involving the 4th power of the hydrodynamic velocity scale and hence, proportional to  $\sigma_h^4$  in any hydrodynamic frequency. Total radiated *power* with spherical spreading at a large distance  $|\mathbf{r}| = \sqrt{x^2 + y^2 + z^2}$  [Eq. (2.2.5) in Howe, 2003] from one eddy is proportional to  $p_a^2$  as

$$P_{FF,rad} \approx \frac{L^2 \rho_0 u^8}{c_a^5} = L^2 \rho_0 u^3 M^5. \quad (6)$$

Lighthill's 8th power law—with a disconcerting sensitivity to  $u$ . This result assumes spherical spreading—absent any reflective ocean boundaries—a major assumption producing a lower bound on the acoustic intensities, but nonetheless indicating the difficulties of scale analyses. The high powers appearing in these formulas suggest some delicacy in estimating amplitudes. Whether a far-field exists in the ocean, in terms of open ocean processes, is not so clear. With boundary turbulence (e.g., Arbic *et al.*, 2009), the idea is more natural.

### B. Spreading

Much of the literature on sound in fluids considers spherical spreading, a major exception being the discussion of sound in acoustic waveguides (e.g., Morse and Ingard, 1968). The appropriate geometry in the oceans is not

obvious. Close to an isolated source, spherical spreading of short acoustic wavelengths would be appropriate. Contact, at any wavelength, with the upper and lower boundaries, raises various questions: a smooth free upper surface at zero pressure would be purely reflective, as would a rigid lid there. Treating surface roughness involves various scattering problems depending upon wavelengths.

A flat seafloor can transmit energy via elastic waves into the solid Earth. Sufficiently efficient transmission processes would render the geometry more like that of a half-space with only the upper boundary present, albeit the impedance change at the bottom would require some reflection. In Sec. III, surface acoustic boundary conditions are ignored, producing a lower bound. The bottom is treated as rigid only in the single eddy case, and no definitive result is claimed.

Additional calculations have been made (not shown) of sound generation by open ocean turbulence and internal waves. The calculations are subject to a large number of sometimes arbitrary assumptions including specifics of the statistics of  $\mathbf{T}$  in various flow types. Thus, the purpose of this present note is to provide a sketch of a much simplified, but perhaps oceanographically relevant, situation.

## III. OCEAN BOUNDARY TURBULENCE

van Haren and Gostiaux (2010) describe a series of Kelvin–Helmholtz billows on a sloping bottom over a large seamount in the ocean. Billows are size 10–15 m in size, appearing in one phase of the tidal oscillations. Could such a phenomenon be detected acoustically? A rough, kinematic representation of those motions is considered. [Howe (1991), analyzed the high frequency acoustics of the boundary layers in free stream turbulence generated in a wind tunnel.]

As a simplified analogue, without statistical assumptions, consider a vortex on a *flat* bottom, with vortex strength  $\Gamma$  (see Lamb, 1932; Milne-Thomson, 1968). Roughly speaking, using the van Haren and Gostiaux (2010) report (Fig. 3 in their report), let the vortex have a diameter of about 10 m. Vortex center is  $a = 15$  m above the bottom. They report movement between vortex centers approximately every 50 s. A stream function satisfying the boundary condition of no normal acoustic velocity across  $z = 0$  for a single vortex is

$$\psi(x, z) = \Gamma \log \frac{\sqrt{(x - x_0)^2 + (z - a)^2}}{\sqrt{(x - x_0)^2 + (z + a)^2}}, \quad (7)$$

where  $x_0$  is the position of the reference vortex above the plane at  $z = 0$ , and  $2a$  is the vertical separation between the vortex and its mirror image across the bottom boundary. For the moment, the vortex extends infinitely far in the  $y$ -direction (Fig. 4) Strength,  $\Gamma$ , controls both the velocity within the vortex, and the speed with which a vortex pair moves in the  $x$ -direction under their mutual interaction.



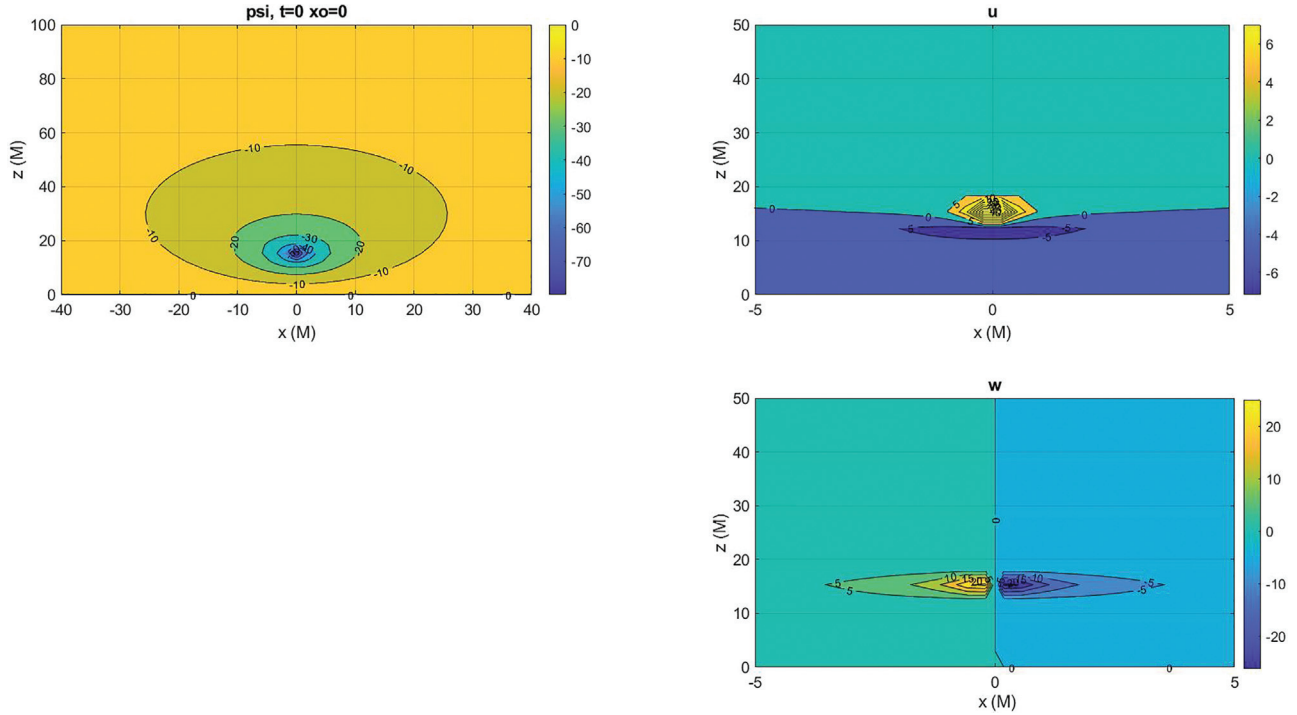


FIG. 4. Stream function (upper left panel,  $m^2/s$ ),  $u$  (upper right), and  $w$  (lower right) in m/s for the mirror image pair of vortices.  $W$ , and hence  $T_{12}$ , is discontinuous across the center. The contouring algorithm exaggerates the size of the small region of intense flow arising from the singularity.

The vortex and its mirror image pair would translate in the  $x$ -direction with a velocity  $dx_0/dt = \Gamma/2a$  m/s which is assumed to be defined by the 50 s interval of [van Haren and Gostiaux \(2010\)](#) for moving an eddy diameter producing with this value of  $a$ ,  $4a^2/\Gamma = 50$ , or  $\Gamma = 18m^2/s$ .

Define

$$D_1(x, z, t) = \sqrt{(x - x_0)^2 + (z - a)^2},$$

$$D_2(x, z, t) = \sqrt{(x - x_0)^2 + (z + a)^2}, \quad (8)$$

and

$$x_0 = \frac{\Gamma}{2a} t. \quad (9)$$

For this single vortex pair, the hydrodynamic velocities are

$$u_h = -\frac{\partial\psi(x, z)}{\partial z} = \Gamma \left( \frac{z - a}{D_1^2} - \frac{z + a}{D_2^2} \right) \quad (10)$$

and

$$w_h = \frac{\partial\psi(x, z)}{\partial x} = \Gamma \left( -\frac{x - x_0}{D_1^2} + \frac{x - x_0}{D_2^2} \right), \quad (11)$$

noting that  $w_h(z = 0) = 0$  as required by the boundary condition (where  $D_1 = D_2$ ). The singularities where  $D_1, D_2 = 0$  are here dealt with pictorially through a crude numerical approximation. Then, the Lighthill tensor matrix components are

$$T_{11} = \rho_0 \Gamma^2 \left\{ \frac{(z - a)}{D_1^2} - \frac{(z + a)}{D_2^2} \right\}^2, \quad (12)$$

$$T_{12} = T_{21} = \rho_0 \Gamma^2 \left\{ \frac{(z - a)}{D_1^2} - \frac{(z + a)}{D_2^2} \right\} \times \left\{ -\frac{(x - x_0)}{D_1^2} + \frac{(x - x_0)}{D_2^2} \right\}, \quad (13)$$

$$T_{22} = \rho_0 \Gamma^2 \left\{ -\frac{(x - x_0)}{D_1^2} + \frac{(x - x_0)}{D_2^2} \right\}^2. \quad (14)$$

$T_{12}$  and  $T_{22}$  vanish at the nominal vortex center,  $x = x_0$ . The 50 s time scale in the velocities implies a 25 s time scale in  $\mathbf{T}$ , or 0.04 Hz (Fig. 5).

The second derivatives of these elements of  $\mathbf{T}$  are readily found as

$$\frac{\partial^2 T_{11}}{\partial x^2} = \rho_0 \frac{\partial^2}{\partial x^2} \left( \frac{\partial\psi}{\partial z} \right)^2 = 2\rho_0 \frac{\partial^3 \psi}{\partial x^2 \partial z}, \quad (15)$$

$$\frac{\partial^2 T_{12}}{\partial x \partial z} = -\rho_0 \frac{\partial^2}{\partial x \partial z} \left( \frac{\partial\psi}{\partial z} \frac{\partial\psi}{\partial x} \right) = \rho_0 \frac{\partial^3 \psi}{\partial x^2 \partial z} + \rho_0 \frac{\partial^3 \psi}{\partial x \partial z^2}, \quad (16)$$

$$\frac{\partial^2 T_{22}}{\partial z^2} = \rho_0 \frac{\partial^2}{\partial z^2} \left( \frac{\partial\psi}{\partial x} \right)^2 = 2\rho_0 \frac{\partial^3 \psi}{\partial x \partial z^2}. \quad (17)$$

Put  $x_0 = 0$  (that is, using a moving coordinate), then  $T_{ij} = O(10^5)$  and the second derivatives are  $O(10^5/a^2)$ .



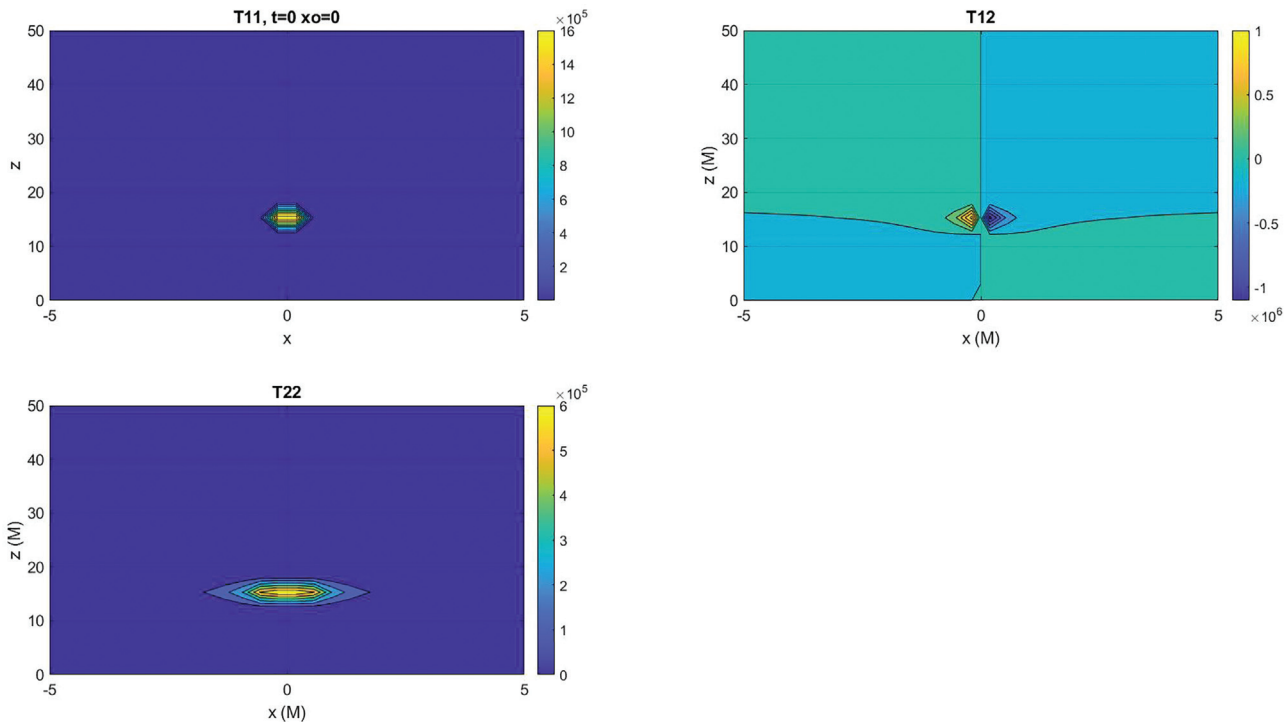


FIG. 5. Elements of  $\mathbf{T}$  in  $\text{kg/m}^2/\text{s}$  for a single vortex over a flat plate ( $T_{11}$  upper left,  $T_{12}$  upper right,  $T_{22}$  lower left). Note that image sources appear in the acoustic problem if the bottom and top are rigid.

## IV. ACOUSTIC WAVE EQUATION

### A. Green function. One vortex

The sound speed,  $c_a$ , is so much larger than any hydrodynamical flow speed, that the acoustic response is essentially instantaneous over even large oceanographic distances. In those cases, the wave equation reduces to the Laplace/Poisson equation. For two dimensions, implying a  $y$ -independent disturbance, the Green function is  $G = -2 \log R$ , and in three-dimensions is  $1/R$ ,  $R = [(x - x')^2 + (y - y')^2 + (z - z')^2]^{1/2}$  (Morse and Feshbach, 1953). Ignoring reflections from the acoustic boundary condition on  $z = 0$ , and the sea surface, these free-space Green functions can be used directly so that

$$p_a(x, y, z, t) = \iiint \mathcal{F}(x', y', z', t) G(x - x', y - y', z - z') \times dx' dy' dz', \quad z' > 0. \quad (18)$$

Sensitivity to treatment of the singularities is evident. Set  $z = 1000$  m,  $x' = 0$ ,  $y' = 0$ , the near-field directly overhead of the vortex at  $t = 0$ , an approximating sum to Eq. (18) has magnitude  $10^{-3}$  Pa in three dimensions, and 5 Pa in two dimensions, again displaying the sensitivity to assumptions. Here the handling of the strong singularities present, and recall, the 8th power law. If the three-dimensional result extends over a  $y$  distance of 1 km, approximately, 1 Pa is obtained for the three-dimensional result. Thus, an estimate of the influence of a single vortex over a flat plane is  $O(1)$  Pa, as compared to a detection threshold of about  $4 \times 10^{-3}$  Pa estimated from Eq. (18) above. It is not obvious how many such vortices would exist simultaneously spread over

the entire ocean basin. To the extent that the sea bottom and surface are rigid, this solution underestimates the magnitude by at least a factor of 2, as it does not account for the acoustic image sources necessary to satisfy both the top and bottom boundary condition (in this case, images of the hydrodynamic vortex and its acoustic image) (Howe, 2003; Morse and Ingard, 1968). Numerical values are well above those seen in the high frequency spectra, as quoted above in Sec. 1A. If 1 Pa of power is distributed over a bandwidth of  $10^{-3} - 10^{-2}$  Hz (Figs. 1 and 3) the power spectral density is approximately  $10^2 \text{ Pa}^2/\text{Hz}$ —the same order as observed. Much larger values would occur if the sound field were generated by basin-scale simultaneous sources.

### B. Vortex street

A different estimate can be based on an infinite row of such vortices (Lamb, 1932). The velocities are

$$u = -\frac{\Gamma}{2a} \frac{\sinh(2\pi z/a)}{\cosh(2\pi z/a) - \cos(2\pi x/a)}, \quad (19)$$

$$w = \frac{\Gamma}{2a} \frac{\sin(2\pi x/a)}{\cosh(2\pi z/a) - \cos(2\pi x/a)},$$

and which for large  $z$ ,  $|u| \rightarrow \Gamma/2a$ ,  $|w| \rightarrow 0$ . (The mirror image across the solid bottom is not included.) van Haren and Gostiaux (2010) suggest of order 10 vortices existing at one time. An infinite street of vortices will move at a speed  $\Gamma/2a \coth(2\pi) \approx \Gamma/2a$  (Batchelor, 1967).  $\Gamma/2a$  is thus still a reasonable estimate of the horizontal displacement velocities. The time scale remains  $4a^2/\Gamma$ , which would be 50 s or

0.02 Hz. The acoustic field, from **T**, will have a frequency twice that value.

## V. DISCUSSION

The intention here has been directed primarily at raising, but only schematically answering, a question: whether oceanographically interesting flow fields produce a measurable acoustic field? A speculative result suggests that boundary turbulence, at least as represented as highly idealized vortices, should be a measurable factor in seismo-acoustic measurement of ocean sound in the low-energy high-frequency range. More generally, acoustic signatures will have far-larger wavelengths than those of the corresponding hydrodynamic fields. For the particular case analyzed, these high frequencies would be modulated by the tidal frequency.

An implication of the result is that the acoustic signature of oceanic noise will have a much larger spatial extent than would the underlying turbulent flow elements. Distinguishing it from, e.g., the disturbances discussed by [Chave et al. \(2019\)](#), would likely require use of large-scale arrays determining the coherence and wavenumber structure as a function of frequency (see [Chave et al., 2019](#), Fig. S4, for a short-distance coherence). Standard beamforming methods could be used, potentially greatly increasing signal-to-noise ratios. The frequency cross-spectral approach of [Howe \(1991\)](#) is a step toward determining wavelengths. Whether the highest frequency structures visible in Fig. 3, with instrument proximity to the Hawaiian Island chain, are connected to the existence of nearby topography is not clear.

The reader will appreciate that boundary turbulence in the ocean is considerably more complex than in the model used here, even over an abyssal plane (see [Munk and Wimbush, 1970](#); [Weatherly and Martin, 1978](#); [Armi and D'Asaro, 1980](#)). Such motions will be additional noise generators, assuming they appear alongside the [van Haren and Gostiaux \(2010\)](#) dynamics. The physics of the Kelvin–Helmholtz billows is also greatly oversimplified here (see, e.g., [Thorpe, 2005](#)), and the calculations reported should be taken as producing only a rough order of magnitude of a lower bound.

Great care must be taken in interpreting the observations of the high frequency, low-energy part of the spectrum, including the hum band. For example, an instrument attached to the seafloor will detect motion of the seafloor itself, and separating a forcing from the coupled response requires vertical information in the water column, information that is not normally available. The physics of both the extremely energetic upper boundary (surface gravity waves in particular) and of the seafloor are complex in their own right. In addition to the problem of microseism generation at the sea surface, coping with seismic movement of the seafloor is necessary. See [Nishida et al. \(2008\)](#) for discussion of the generation and propagation of Love and Rayleigh waves in the ocean basins. A further complication is the self-noise generated by flow past the instrument. Mid-water, beamforming, arrays of instruments,

such as that envisioned by [Simons et al. \(2019\)](#), are an attractive alternative to bottom-coupled instruments. In any case, as would follow from the analysis above, discrimination in acoustic wavenumbers and horizontal propagation directions are likely to be the simplest test of these and competing ideas.

The mathematics of the Lighthill generation mechanism is in principle straightforward, but in practice, results in cumbersome and sensitive algebraic structures that are not so easy to interpret. This problem appears to be one where numerical models, able to span the full range of oceanic motions, at least regionally, and coupled directly to the acoustic wave equation, represent the most likely path to better understanding.

To the extent that any of this proves to be practical, an interesting hypothetical future application would be to understand the fluid flow in the ice-covered oceans of the outer solar system moons such as Enceladus and Europa (see [Jansen, 2016](#)). It is possible to envision lowering a hydrophone array through the ice and determining the flow fields by listening to them. The background noise might be much reduced: no waves, little seismicity, and no marine mammals.

## ACKNOWLEDGMENTS

The author thanks A. Chave for providing the HOME data. Comments and corrections from three anonymous reviewers and O. A. Godin are appreciated. Partial support came from the Cecil and Ida Green Chair at MIT.

- Arbic, B. K., Muller, M., Richman, J. G., Shriver, J. F., Morten, A. J., Scott, R. B., Serazin, G., and Penduff, T. (2014). "Geostrophic turbulence in the frequency-wavenumber domain: Eddy-driven low-frequency variability," *J. Phys. Oceanogr.* **44**, 2050–2069.
- Arbic, B. K., Shriver, J. F., Hogan, P. J., Hurlburt, H. E., McClean, J. L., Metzger, E. J., Scott, R. B., Sen, A., Smedstad, O. M., and Wallcraft, A. J. (2009). "Estimates of bottom flows and bottom boundary layer dissipation of the oceanic general circulation from global high-resolution models," *J. Geophys. Res. Oceans* **114**, C02024, <https://doi.org/10.1029/2008JC005072>.
- Ardhuin, F., and Herbers, T. H. C. (2013). "Noise generation in the solid Earth, oceans and atmosphere, from nonlinear interacting surface gravity waves in finite depth," *J. Fluid Mech.* **716**, 316–348.
- Armi, L., and D'Asaro, E. (1980). "Flow structures of the benthic ocean," *J. Geophys. Res.: Oceans* **85**, 469–484, <https://doi.org/10.1029/JC085iC01p00469>.
- Batchelor, G. K. (1967). *Introduction to Fluid Dynamics* (Cambridge University Press, Cambridge, UK), p. 615.
- Chave, A. D., Luther, D. S., and Thomson, D. J. (2019). "High-*Q* spectral peaks and nonstationarity in the deep ocean infragravity wave band: Tidal harmonics and solar normal modes," *J. Geophys. Res. Oceans* **124**, 2072–2087, <https://doi.org/10.1029/2018JC014586>.
- Colosi, J. A. (2015). *Sound Propagation through the Stochastic Ocean* (Cambridge University Press, Cambridge, UK).
- Diaz, J. (2016). "On the origin of the signals observed across the seismic spectrum," *Earth-Sci. Rev.* **161**, 224–232.
- Ferrari, R., and Wunsch, C. (2009). "Ocean circulation kinetic energy: Reservoirs, sources, and sinks," *Annu. Rev. Fluid Mech.* **41**, 253–282.
- Filloux, J. H. (1980). "Pressure-fluctuations on the open ocean-floor over a broad frequency-range-new program and early results," *J. Phys. Oceanogr.* **10**, 1959–1971.
- Gregg, M. C. (2021). *Ocean Mixing* (Cambridge University Press, Cambridge, UK).

- Haver, S. M., Gedamke, J., Hatch, L. T., Dziak, R. P., Van Parijs, S., McKenna, M. F., Barlow, J., Berchok, C., DiDonato, E., Hanson, B., Haxel, J., Holt, M., Lipski, D., Matsumoto, H., Meinig, C., Mellinger, D. K., Moore, S. E., Oleson, E. M., Soldevilla, M. S., and Klinck, H. (2018). "Monitoring long-term soundscape trends in U.S. waters: The NOAA/NPS Ocean Noise Reference Station Network," *Mar. Pol.* **90**, 6–13.
- Howe, B. M., Miksis-Olds, J., Rehm, E., Sagen, H., Worcester, P. F., and Haralabus, G. (2019). "Observing the oceans acoustically," *Front. Mar. Sci.* **6**, 426.
- Howe, M. S. (1991). "Surface pressures and sound produced by turbulent flow over smooth and rough walls," *J. Acoust. Soc. Am.* **90**, 1041–1047.
- Howe, M. S. (2003). *Theory of Vortex Sound* (Cambridge University Press, New York).
- Jansen, M. F. (2016). "The turbulent circulation of a snowball Earth ocean," *J. Phys. Oceanogr.* **46**, 1917–1933.
- Jensen, F. B., Kuperman, W. A., Porter, M. B., and Schmidt, H. (2011). *Computational Ocean Acoustics*, 2nd ed. (Springer, New York).
- Kraichnan, R. H. (1957). "Relation of fourth-order to second-order moments in stationary isotropic turbulence," *Phys. Rev.* **107**, 1485–1490.
- Lamb, H. (1932). *Hydrodynamics*, 6th ed. (Dover, New York).
- Lighthill, M. J. (1952). "On sound generated aerodynamically I. General theory," *Proc. R. Soc. A* **211**, 564–587.
- Lighthill, M. J. (1954). "On sound generated aerodynamically II. Turbulence as a source of sound," *Proc. R. Soc. A* **222**, 1–32.
- Medwin, H., and Blue, J. E. (2005). *Sounds in the Sea: From Ocean Acoustics to Acoustical Oceanography* (Cambridge University Press, New York).
- Milne-Thomson, (1968). *Theoretical Hydrodynamics* (Macmillan, New York). **Xxii**, p. 743.
- Möhring, W. (1979). "General lecture: Modelling low mach number noise," in *Mechanics of Sound Generation in Flows*, edited by E. A. Müller (Springer-Verlag, Berlin), pp. 85–96.
- Monin, A. S., and Yaglom, A. M. (1975). *Statistical Fluid Mechanics: Mechanics of Turbulence*, translated from the Russian edition of 1965 (The MIT Press, Cambridge, USA), Vol. 2, Chaps. 7 and 11.
- Morse, P. M., and Feshbach, H. (1953). *Methods of Theoretical Physics* (McGraw-Hill, New York), Vol. 2.
- Morse, P. M., and Ingard, K. U. (1968). *Theoretical Acoustics* (Princeton University Press, Princeton, NJ).
- Moum, J. N. (2021). "Variations in ocean mixing from seconds to years," *Annu. Rev. Mar. Sci.* **13**, 201–226.
- Müller, E. A. (1979). "Mechanics of sound generation in flows: Joint symposium Gottingen/Germany," in *Max-Planck-Institut für Stromungsforschung*, August 28–31, Berlin (Springer-Verlag, New York).
- Munk, W., and Wimbush, M. (1970). "The benthic boundary layer," *The Sea* **4**, 731–758.
- Munk, W., Worcester, P., and Wunsch, C. (1995). *Ocean Acoustic Tomography* (Cambridge University Press, Cambridge, UK).
- Nishida, K. (2013). "Earth's background free oscillations," *Annu. Rev. Earth Planet. Sci.* **41**, 719–740.
- Nishida, K., Kawakatsu, H., Fukao, Y., and Obara, K. (2008). "Background Love and Rayleigh waves simultaneously generated at the Pacific Ocean floors," *Geophys. Res. Lett.* **35**, L16307, <https://doi.org/10.1029/2008GL034753>.
- Proudman, I. (1952). "The generation of noise by isotropic turbulence," *Proc. R. Soc. London A* **214**, 119–132.
- Thorpe, S. A. (2005). *The Turbulent Ocean* (Cambridge University Press, New York).
- Simons, F. J., Simon, J. D., Hello, Y., Nolet, G., Obayashi, M., and Chen, Y. J. (2019). "EarthScope-Oceans: An array of floating MERMAID instruments for earthquake seismology," *J. Acoust. Soc. Am.* **146**, 3067.
- Vallis, G. K. (2017). *Atmospheric and Oceanic Fluid Dynamics: Fundamentals and Large-Scale Circulation* (Cambridge University Press, Cambridge, UK).
- Van Haren, H., and Gostiaux, L. (2010). "A deep-ocean Kelvin-Helmholtz billow train," *Geophys. Res. Lett.* **37**, L03605, <https://doi.org/10.1029/2009GL041890>.
- Weatherly, G. L., and Martin, P. J. (1978). "On the structure and dynamics of the oceanic bottom boundary layer," *J. Phys. Oceanogr.* **8**, 557–570.
- Webb, S. C. (2008). "The Earth's hum: The excitation of Earth normal modes by ocean waves," *Geophys. J. Intern.* **174**, 542–566.
- Wenz, G. M. (1962). "Acoustic ambient noise in the ocean: Spectra and sources," *J. Acoust. Soc. Am.* **34**, 1936–1956.
- Wu, W., Zhan, Z., Peng, S., Ni, S., and Callies, J. (2020). "Seismic ocean thermometry," *Science* **369**, 1510–1515.
- Wunsch, C. (2020). "Is the ocean circulation speeding up? Ocean surface trends," *J. Phys. Oceanogr.* **50**, 3205–3217.